

A cis-replication element functions in both orientations to enhance replication of *Turnip crinkle virus*

Xiaoping Sun, Anne E. Simon*

Department of Cell Biology and Molecular Genetics, Microbiology Building, University of Maryland College Park, College Park, MD 20742, USA

Received 2 November 2005; returned to author for revision 14 December 2005; accepted 14 March 2006

Available online 6 June 2006

Abstract

Turnip crinkle virus (TCV) (family *Tombusviridae*, genus *Carmovirus*) is a positive-sense RNA virus containing a 4054-base genome. Previous results indicated that insertion of Hairpin 4 (H4) into a TCV-associated satellite RNA enhanced replication 6-fold in vivo (Nagy, P., Pogany, J., Simon, A. E., 1999. *EMBO J.* 18:5653–5665). A detailed structural and functional analysis of H4 has now been performed to investigate its role in TCV replication. RNA structural probing of H4 in full-length TCV supported the sequence forming hairpin structures in both orientations in vitro. Deletion and mutational analyses determined that H4 is important for efficient accumulation of TCV in protoplasts, with a 98% reduction of genomic RNA levels when H4 was deleted. In vitro transcription using p88 [the TCV RNA-dependent RNA polymerase] demonstrated that H4 in its plus-sense orientation [H4(+)] caused a nearly 2-fold increase in RNA synthesis from a core hairpin promoter located on TCV plus-strands. H4 in its minus-sense orientation [H4(-)] stimulated RNA synthesis by 100-fold from a linear minus-strand promoter. Gel mobility shift assays indicated that p88 binds H4(+) and H4(-) with equal affinity, which was substantially greater than the binding affinity to the core promoters. These results support roles for H4(+) and H4(-) in TCV replication by enhancing syntheses of both strands through attracting the RdRp to the template.

© 2006 Elsevier Inc. All rights reserved.

Keywords: RNA-dependent RNA polymerase; RNA virus replication; RNA enhancer; Turnip crinkle virus; cis-acting replication element

Introduction

Positive-strand RNA viruses use similar strategies for replicating their genomes. After invading the host cell, the viral genome is released from the capsid, recruited by ribosomes, and then translated to produce the RNA-dependent RNA polymerase (RdRp). The genomic RNA then serves as template for transcription of complementary minus-strands by the replicase complex, which comprises the RdRp and possibly other viral or host factors (Lai, 1998). Newly synthesized minus-strands are then used as templates for synthesis of large quantities of progeny plus-strands. The relative levels of the two strands are often highly asymmetric, with ratios of up to 1000 plus-strands for every minus-strand produced (Buck, 1996).

Viral RdRps must recognize their cognate RNA through direct or indirect interaction with specific sequence or structural elements located on the template. The RNA elements can be

hairpins, pseudoknots, tRNA-like structures, cloverleaf-like structures or short primary sequences without apparent high-order structure (Dreher, 1999). Using in vivo and in vitro approaches, core promoter elements located proximal to the 3' terminus have been identified that contain specific sequence and/or structural features needed for recognition by the RdRp (Buck, 1996; Chapman and Kao, 1999; Dreher, 1999; Duggal et al., 1994; Turner and Buck, 1999).

In addition to core promoters, many RNA viruses contain cis-acting elements that enhance or repress RNA synthesis (Kim and Makino, 1995; Nagy et al., 1999; Panavas and Nagy, 2003; Panavas and Nagy, 2005; Pogany et al., 2003; Ray and White, 1999, 2003; Zhang et al., 2004). Enhancers, which have generally been identified in minus-strands, are thought to help recruit the RdRp to the template. Elements that repress transcription in vitro and are required in vivo have recently been identified for two members of the family *Tombusviridae*. These elements are hairpins located just upstream from the core promoter in plus-strands, which pair with 3'-terminal sequences and are proposed to shield these sequences from the RdRp

* Corresponding author. Fax: +1 301 805 1318.

E-mail address: simona@umd.edu (A.E. Simon).

RNA recombination in vivo (Carpenter et al., 1995; Cascone et al., 1993). Altogether, these results led to the suggestion that M1H functioned primarily in its minus-sense orientation as a replication enhancer.

While preliminary evidence indicates that M1H and H4 are functionally related, the proximity of H4(+) to the 3' proximal elements H4a/H4b/H5/Pr suggested that H4(+) might also be important for minus-strand synthesis. *Cardamine chlorotic fleck virus* (CCFV), which shares 41% sequence similarity with TCV in their 3' UTR, has a nearly identical H4 in the same location, except for a GC to CG exchange in the middle stem and a U to G transversion in the terminal loop. These observations suggest an important sequence-specific role for H4 in TCV and CCFV accumulation that might reflect functions in both orientations.

We now provide evidence for involvement of H4(+) and H4(-) in replication of TCV. Disruption of its structure or alteration of its internal or terminal loop sequences caused substantially reduced accumulation of TCV in *Arabidopsis* protoplasts. In vitro RNA transcription and gel mobility shift assays using *E. coli*-expressed p88 indicated that both H4(+) and H4(-) have enhancer activity and both bind RdRp with similar affinity that was substantially greater than the binding affinity of the RdRp for the core promoters. This suggests that H4(+) and H4(-) function to enhance plus- and minus-strand synthesis by attracting the RdRp to the TCV genomic RNA template.

Results

Solution structure probing of the H4 region in TCV plus and minus strands

The sequence and structural conservation of TCV and CCFV H4 suggests that H4(+) and/or H4(-) exist as stem-loop structures. To determine if the H4(+) hairpin is present on plus-strands, RNA solution structural probing was performed by subjecting TCV full-length plus-strand transcripts to chemical and enzymatic probing in vitro. Transcripts were subjected to partial treatments with DMS (methylates the N1 and N3 positions of unpaired adenylates and cytidylates, respectively), RNase T1 (cleaves at single-stranded guanylates), RNase A (cleaves at single-stranded pyrimidines) and RNase V1 (cleaves at double-stranded and stacked residues). The location of cleaved or modified bases was determined following primer extension and electrophoresis through 6% sequencing gels (Fig. 2A).

For H4(+), five of the six bases comprising the internal asymmetric loop were recognized by various single-strand-specific reagents, strongly suggesting that this loop is unpaired. In the terminal loop, G3879, U3883, and A3884 were accessible to single-strand-specific reagents, while five of the remaining six positions (3881–3882, 3886–3888) had premature polymerase termination sites in the absence of treatment and thus could not be evaluated. The predicted upper stem contained one strong and three weak RNase V1 signals, while C3873 adjacent to the interior asymmetric loop was susceptible to RNase A, suggesting breathing at the base of the stem. The bases flanking both sides of H4(+) were strongly susceptible to single-strand-

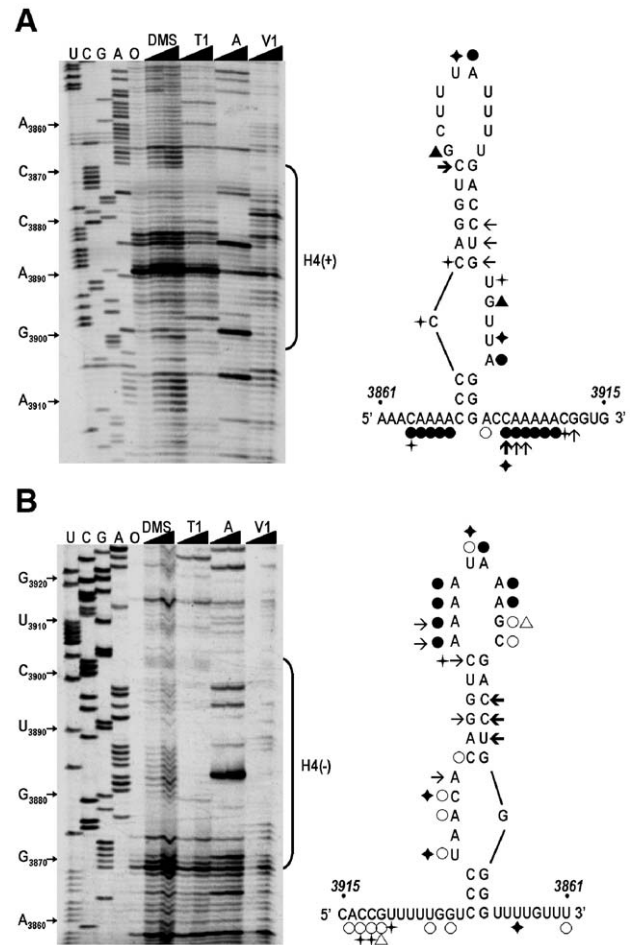


Fig. 2. Chemical and enzymatic probing of H4(+) and H4(-). TCV plus-strand transcripts (A) or minus-strand transcripts (B) were treated with DMS for 10 or 20 min or with RNase T1, RNase A and RNase V1 for 5 or 10 min. The modified or cleaved RNAs were subjected to primer extension using an oligonucleotide complementary to positions 3950 to 3970 of TCV genomic RNA (A) or homologous to positions 3773 to 3789 for minus-strand extension in (B). Left panels, representative gel showing H4 and surrounding sequence. The region corresponding to H4 is indicated. The sequencing ladder comprises the first four lanes. Bases corresponding to specific nucleotides are indicated at left. "0" indicates sample that was not treated with reagents prior to primer extension. Solid triangles above lanes indicate increasing incubation time. Right panels (A and B), summary of solution structure probing. Low or high sensitivity to reagents is indicated by open or solid symbols, respectively, or by light or bold arrows, respectively. Circles, DMS; triangles, RNase T1; stars, RNase A; arrows, RNase V1.

specific reagents, with positions 3905–3807 and 3912 also cleaved by RNase V1. This suggests either that these residues are structurally flexible due to the formation of alternative or tertiary RNA structures. All together, these results are consistent with the computer-predicted and phylogenetically conserved H4(+) structure.

Solution structure probing was also performed on TCV full-length minus-strands to examine if H4(-) also exists as a hairpin. As shown in Fig. 2B, most residues in the loop region were recognized by DMS, RNase T1, or RNase A, and thus are likely single-stranded. One adenylate in the internal loop and two adenylates in the terminal loop were recognized by RNase V1, suggesting that these bases are stacked or may pair with

another region. The upper stem was recognized by RNase V1, producing three strong and two weak signals, while C3889 and C3894, which are adjacent to the terminal and internal loop, respectively, were susceptible to single-stranded specific reagents. In this experiment, some uridyates and guanylates were weakly susceptible to DMS for unknown reasons. Taken together, the probing data for TCV minus-strands was consistent with the predicted H4(-) structure, suggesting that the sequence forms a hairpin in both strands.

H4 is important for efficient accumulation of TCV in vivo

H4(-) is a hot spot for reinitiation of transcription by the RdRp during the process of RNA recombination, which results in the joining of full-length or nearly full-length satD to the 3' region of TCV (Carpenter et al., 1995). Since recombination hotspots attract RdRp to the acceptor strand and have enhancer activity (Nagy et al., 1999; Cheng et al., 2005), it seemed likely that TCV H4(-) serves as an enhancer of TCV replication. However, the location of H4(+) just upstream from the plus-sense 3' proximal hairpins H4a/H4b/H5/Pr suggests that H4(+) may perform a related role in minus-strand synthesis.

To examine how H4 participates in viral accumulation, H4 was deleted or subjected to site-specific mutations (Fig. 3A). Transcripts of TCV H4 mutants were inoculated into protoplasts and total RNA extracted at 40 h postinoculation (hpi) was analyzed by RNA gel blots (Fig. 3B). Deletion of H4 (construct M1) reduced plus-strand RNA accumulation to 2% of wt TCV levels indicating that H4 is important for efficient accumulation of TCV. To confirm the importance of the hairpin structure, a middle position of the upper six base stem (G3876–C3891) was altered to a G G mismatch (construct M2) or a C C mismatch (construct M3). M2 and M3 showed only slight reductions in accumulation (to 82–90% of wt TCV), while a compensatory G–C to C–G exchange at this position (construct M4) increased plus-strand accumulation to wt levels.

Since it was possible that the six base H4 stem might not be fully disrupted by eliminating a canonical base-pair in a central position, two additional constructs were generated that simultaneously disrupted two base-pairs in the stem, A3874–U3893 and U3877–A3890. Disrupting these pairs by converting A3874 to U and U3877 to A (construct M5) or A3890 to U and U3893 to A (construct M6) decreased plus-strand accumulation to 2% of wt TCV levels (Fig. 3B). When both pairings were re-established with compensatory changes (construct M7), accumulation of plus-strands was restored to wt TCV levels. These results establish the importance of the larger H4 stem, which was likely not substantially affected by disruption of a single central position. This is similar to a previous finding with H5, where disruption of the central C–G pairing in the three base stem of satC H5 was detrimental, while disruption of the same base-pair in satC with H5 of TCV, which contains a five base stem in this location, did not affect satC accumulation (Zhang and Simon, 2005).

To evaluate the importance of the three base lower stem, the center position (C3870–G3901) was altered to a C C mismatch (construct M15) or a G G mismatch (construct M16). M15 and M16 plus strands did not accumulate to detectable levels, while a compensatory C–G to G–C exchange at this position (construct M17) restored plus-strand accumulation to 80% of wt levels. All together, these results confirm the RNA solution structure assays and mFold structural predictions for the H4(+) structure depicted in Fig. 3A.

We next examined the importance of the H4 terminal and interior loops as well as H4 3' flanking sequences on TCV accumulation. Altering two residues in the asymmetric internal loop (construct M10) or four base changes in the terminal loop (construct M11) reduced levels of plus-strands to about 10% of wt levels, indicating important functions for the H4 single-stranded regions (Fig. 3B). Deleting five consecutive adenylates flanking the 3' side of H4(+) (construct M12) was strongly inhibitory with no TCV detected. To determine whether the

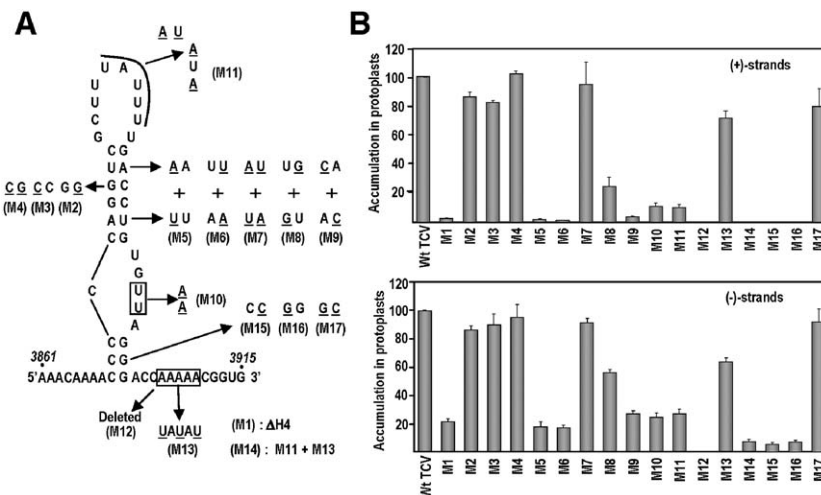


Fig. 3. Mutational analysis of H4. (A) Locations of mutations introduced into the H4 region. Names of constructs are given in parentheses. Nucleotide substitutions are underlined. (B) Accumulation of wt and mutant viral RNAs in protoplasts. Arabidopsis protoplasts were inoculated with transcripts of wt TCV and the H4 mutants. Total RNA was extracted at 40 hpi and subjected to RNA gel blot analysis using an oligonucleotide probe complementary to either plus or minus-strands.

missing bases were sequence specific or required as a spacer between elements, three of the adenylates were converted to uridylates (construct M13). In addition, to explore the possibility that these residues might participate in a pseudoknot with uridylates in the terminal loop, M13 mutations and M11 mutations were combined into a single construct (M14), which would re-establish putative pairing between the two locations. M13 accumulated to 72% of wt while M14 did not reach detectable levels. These results suggest that the spacing between H4(+) and downstream elements, which was altered in M12, and not the identity of the five adenylates, is critical for TCV accumulation.

For nearly all constructs with mutations that significantly reduced levels of TCV plus-strands (M1, M5, M6, M10, M11, M14, M15, M16), accumulation of minus-strands exceeded the accumulation of plus-strands (when compared with wt levels) (Fig. 3B, bottom). For example, deletion of H4 (construct M1) resulted in plus-strand levels that reached only 2% of wt while minus-strand levels were 22% of wt, an 11-fold difference. This differential accumulation in plus- and minus-strands was not reflected in construct M13, which had alterations in sequence flanking H4. While reduced accumulation of plus-strands compared with minus-strands is generally interpreted as an indication of a minus-sense element functioning in plus-strand synthesis, recent findings when altering plus-sense hairpins H5 and H4b in satC indicated similar asymmetric effects on accumulation of plus and minus-strands (Zhang and Simon, 2005; Zhang et al., submitted for publication). Since H5 and the related Tombusvirus hairpin SL3 have been proposed to be sites of replicase organization (McCormack and Simon, 2004; Panaviene et al., 2004; 2005), this led to the suggestion that altering these elements disrupted the interacting replicase, which was more consequential for plus-strand synthesis (Zhang and Simon, 2005).

To gain further insights on whether one or both hairpin orientations function in TCV accumulation, A3874 and A3890 in the upper stem were replaced with guanylates to allow for G–

U pairings at these positions in plus-strands, and C A mismatches in minus-strands (construct M8). M8 plus-strands accumulated to 25% of wt TCV levels while minus-strands reached 56% of wt TCV levels. This reduction could either reflect inability of H4(+) to function properly with two G–U pairings in the stem or that disruption of H4(–) affects TCV accumulation. When U3877 and U3893 were replaced by cytidylates, allowing for C A mismatches in plus-strands and G–U pairings in minus-strands, (construct M9), TCV plus- and minus-strand accumulation was reduced to 4% and 27% of wt, respectively. These results indicate that disruption of H4(+) was more consequential to virus accumulation than H4(–). Since disruption of H4(+) while retaining the structure of H4(–) was less detrimental than disruption of the stem in both orientations (M5 and M6), this suggests that H4(–) is also contributing to TCV accumulation in vivo.

H4 enhances replication of TCV RNAs

While site-specific mutagenesis and deletion analyses indicated that H4 is important for efficient accumulation of TCV in vivo, these experiments did not address if H4 is involved in replication or translation. To begin addressing this question, we made use of the ability of TCV to support the replication of non-coding subviral RNAs, which are frequently used as models to study replication-specific elements (Nagy et al., 1999, 2001; Ray and White, 2003; Fabian et al., 2003). Since H4 is not a component of any natural TCV subviral RNA, it was inserted into the central portion of two artificial non-coding RNAs, TT and CT (Fig. 4A). TT was constructed by joining the 5' end region of TCV (positions 1 to 178) to the 3' 152 bases of TCV (sequence downstream from H4). CT contained the same 3' segment joined to a satC 5' fragment (positions 1 to 176) (Fig. 4A). Wt H4 and H4 with the terminal loop mutations from construct M11 were inserted into the central region of both constructs, producing TT–H4, TT–H4_{M11}, CT–H4 and CT–H4_{M11} (Fig. 4A).

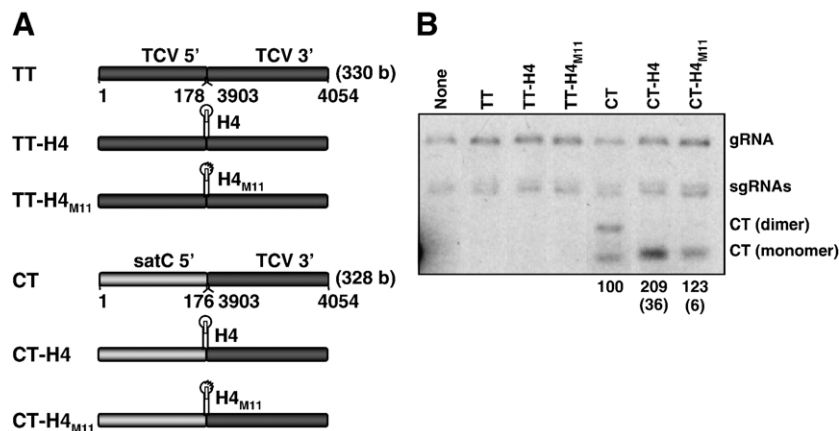


Fig. 4. Effect of H4 on replication of artificial non-coding subviral RNAs. (A) Schematic representation of two artificial subviral RNAs and their derivatives generated by insertion of H4 or H4_{M11}. Numbers denote boundaries of segments derived from TCV or satC. (B) Accumulation of the non-coding RNAs in protoplasts. Total RNA was extracted at 40 hpi and subjected to RNA gel blot analyses using an oligonucleotide probe complementary to the 3' end of TCV. Averaged levels of the accumulating CT RNAs from three independent experiments are given below each lane. Numbers in parentheses denote standard deviations. gRNA, TCV genomic RNA; sgRNAs, TCV subgenomic RNAs.

Transcripts of all constructs were inoculated onto protoplasts with TCV variant CPmT (Wang and Simon, 1999). CPmT contains alterations at the CP translation initiation site that eliminate translation of CP, which allows for enhanced accumulation of subviral RNAs with TCV-related Pr elements (Kong et al., 1995; 1997). Total RNAs were extracted at 40 hpi and analyzed by RNA gel blots (Fig. 4B). No TT construct accumulated to detectable levels while construct CT generated both monomers and dimers, similar to satC. CT–H4 monomers accumulated 2-fold more than CT monomers, indicating that H4 enhances accumulation of this artificial construct. Alterations in the H4 terminal loop that reduced accumulation of TCV also decreased levels of CT–H4 by nearly 60% (construct CT–H4_{M11}). Interestingly, the presence of H4 had a negative effect on levels of dimers, similar to previous observations for satC M1H. While these

results do not exclude a role for H4 in translation, they do indicate that H4 enhances replication of CT, and by analogy, TCV.

H4(+) and H4(–) have enhancer activity in vitro

In vitro transcription by the TCV p88 RdRp was used to determine if both H4(+) and H4(–) can enhance the activity of TCV core promoters. The root constructs contained either the plus-strand Pr core promoter (Song and Simon, 1995) or the minus-strand 3' terminal Carmovirus Consensus Sequence (CCS; C_{2–3}A/U_{3–7}) (Guan et al., 2000). The promoters were flanked by their natural sequences (12 bases for Pr [link1] and 24 bases for CCS [link2]) joined to either wt or mutant H4(+), H4(–) or randomized H4(+) or H4(–) sequence (Rd1 or Rd2, respectively; Fig. 5A).

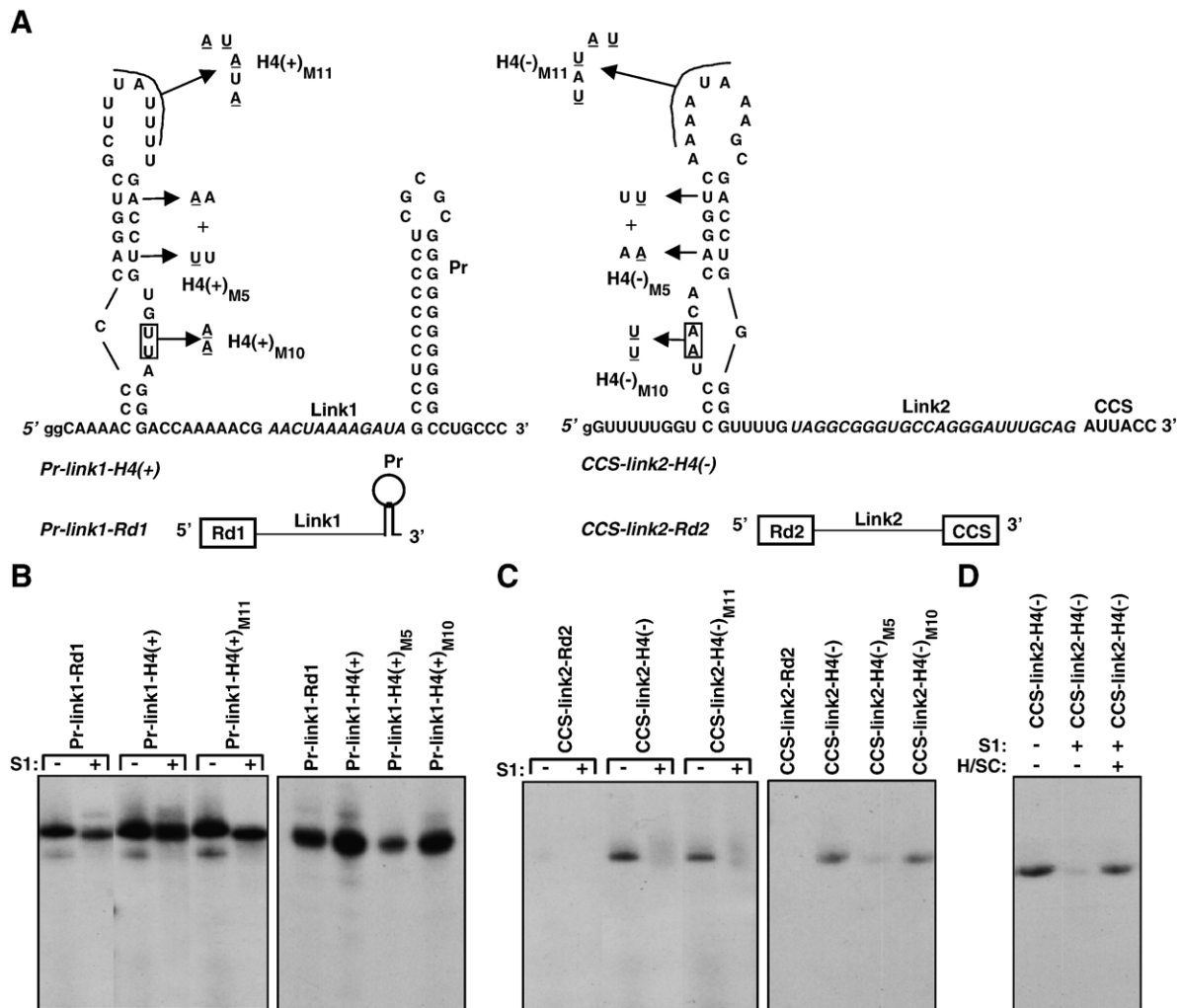


Fig. 5. Effect of H4 on transcription in vitro using recombinant p88. (A) Composition of RNA constructs. Rd1 and Rd2 denote randomized H4(+) and H4(–) sequences, respectively. Bases in lower case were included for efficient transcription by T7 RNA polymerase. Names of mutant constructs containing alterations in H4 are shown as subscripts. (B) In vitro transcription of Pr-containing constructs. Products in the left panel were either untreated (–) or treated (+) with S1 nuclease. (C) In vitro transcription of CCS-containing constructs. Products in the left panel were either untreated or treated with S1 nuclease. (D) Determination that products synthesized from the CCS promoter are single-stranded. After in vitro transcription of CCS-link2-H4(–) with p88, the reaction mix was either untreated, treated with S1 nuclease, or subjected to heating and slow cooling (H/SC) to anneal any de novo synthesized product with template followed by treatment with S1 nuclease. A weak band was visible in the CCS-link2-Rd2 lane in the absence of S1 nuclease treatment in the original autoradiogram. All constructs were tested in three independent assays with very similar results.

H4(+) was a weak enhancer of the plus-strand Pr promoter, augmenting transcription by nearly 2-fold (Fig. 5B). Enhancer activity of H4(+) was not affected by mutations in either the terminal loop [Pr-link1-H4(+)_{M11}] or the internal loop [Pr-link1-H4(+)_{M10}], however, disruption of the upper H4(+) stem eliminated enhancer activity [Pr-link1-H4(+)_{M5}]. In contrast, H4(-) was a very strong enhancer of the minus-strand CCS promoter, enhancing transcription over 100-fold compared with randomized sequence [compare CCS-link2-H4(-) with CCS-link2-Rd2, Fig. 5C]. As with H4(+), mutations in the terminal and internal loops did not affect H4(-) enhancer activity while disruption of the stem substantially reduced enhancer activity. These results indicate that both H4(+) and H4(-) are able to enhance activity of core TCV promoters. Furthermore, the single-stranded sequences in H4, which when disrupted in the context of full-length TCV (Fig. 3) or CT constructs (Fig. 4) affect accumulation, do not impact on the ability of H4(+) and H4(-) to enhance the activity of core promoters in vitro.

Initially, transcripts synthesized by p88 were either not further treated or treated with single-stranded specific S1

nuclease to determine the nature (single-stranded or double-stranded) of the products (Figs. 5B and C, left panels). Treatment of three different products transcribed from the Pr promoter with S1 nuclease only slightly reduced transcript levels, indicating that products were mainly double-stranded as previously found for all RdRp products tested using satC promoters (Nagy et al., 2001). However, CCS-generated products were S1-sensitive, suggesting that these products might be single-stranded. To eliminate the possibility that the RdRp was serving as a terminal transferase and adding radiolabeled nucleotides to the 3' end of the template (which would remain single-stranded and thus degraded by S1 nuclease), template CCS-link2-H4(-) and products were heated and slow cooled to promote annealing prior to S1 nuclease treatment. If de novo synthesized full-length products had been synthesized by the RdRp in the reaction, then this treatment should anneal templates and products into S1 nuclease-resistant double-stranded RNAs (since only a small percentage of available templates are transcribed by the RdRp in vitro, all products should theoretically be able to pair with templates).

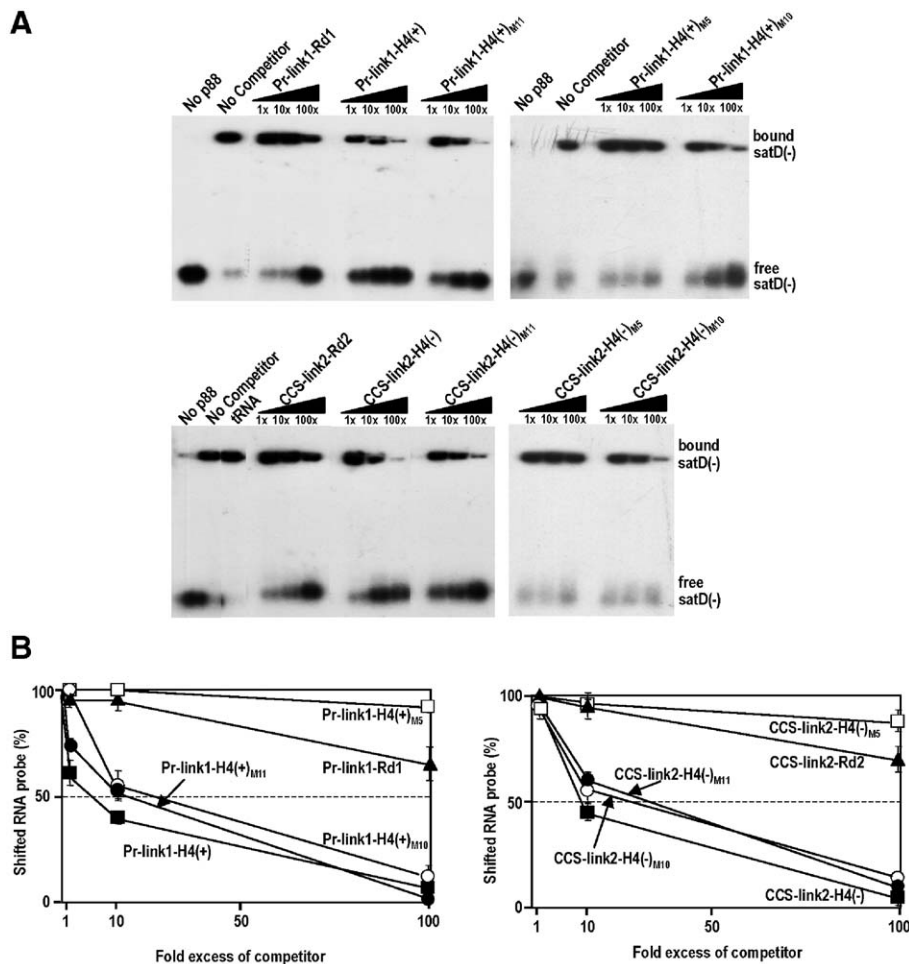


Fig. 6. Preferential binding of p88 to H4(+) and H4(-). (A) Representative gel mobility shift gels of ³²P-labeled satD(-) RNA probe bound to p88 in the absence or presence of unlabeled competitor RNAs described in Fig. 5A. No p88, without added p88; no competitor, ³²P-labeled satD(-) probe alone. 100-fold excess yeast tRNA was used as a non-specific binding control as shown in the lower panel. The two right panels represent portions of the same experiment and are separated for clarity in data presentation. Thus, the controls in the top panel apply to the lower panel. (B) Graphic presentation of data obtained in panel A and one additional independent experiment. The relative levels of the shifted probes were averaged and shown as percentage of the probe level shifted by p88 in the absence of competitor.

However, if radiolabeled nucleotides had been added to the template by terminal transferase activity, the template-derived products should remain single-stranded and be S1 nuclease sensitive. As shown in Fig. 5D, heating and slow-cooling the reaction mix resulted in 87% of the products becoming S1 nuclease resistant. These results indicate that products transcribed from the CCS promoter were synthesized by de novo initiation and were single-stranded.

p88 binds to H4(+) and H4(-)

Our finding that H4(+) and H4(-) can enhance transcription from core promoters suggests that these hairpins might function by binding the RdRp and thus attracting the replicase to the template. To test the validity of this hypothesis, we used a competition assay programmed with radiolabeled satD minus-strands [satD(-)], which are efficiently bound by TCV p88 (Rajendran et al., 2002). To test whether p88 binds to H4(+) and/or H4(-), the constructs described in Fig. 5A were added in one, ten and 100-fold molar excess to fixed levels of the satD(-) probe and purified p88. Competitiveness for binding was determined using gel mobility shift assays. Yeast tRNA, a poor competitor in previous competition experiments (Rajendran et al., 2002), was used as a control.

One hundred-fold molar excess of Pr-link1-Rd1 only reduced satD(-) binding by about 30%, indicating that the TCV Pr is a poor competitor for RdRp binding compared with the satD(-) probe (Fig. 6). In contrast, 10-fold molar excess of Pr-link1-H4(+) reduced satD(-) binding by approximately 50%, indicating that H4(+) binds the RdRp more strongly than the Pr core promoter. Mutations in the H4(+) interior or terminal loops [Pr-link1-H4(+)_{M10} and Pr-link1-H4(+)_{M11}] did not reduce RdRp binding to H4(+), which supports the RdRp transcription results indicating these regions do not affect H4(+) enhancer activity (Fig. 5B). Pr-link1-H4(+)_{M5} was less effective at reducing satD(-) binding compared with Pr-link1-Rd1, consistent with its weaker activity in the in vitro transcription assays (Fig. 5B).

Results with the CCS promoter constructs were very similar to the Pr constructs. CCS was also a weak competitor for RdRp binding (CCS-link2-Rd2; Fig. 6) as was CCS-link2-H4(-)_{M5}. Constructs containing wt H4(-) competed as effectively as constructs containing H4(+), and terminal or interior loop mutations (CCS-link2-M₁₀ and CCS-link2-M₁₁) had no apparent effect on binding. These results indicate that H4(+) and H4(-) have similar affinities for the RdRp in vitro. In addition, alternations in the loop sequences do not affect RdRp binding and thus must disrupt an ancillary function of the hairpin.

Discussion

In this study, we examined the function of TCV hairpin H4, which is structurally similar to the satC enhancer M1H and located in a similar position relative to the 3' end (Nagy et al., 1999). Solution structure analyses suggest that H4 exists as stem-loop structures in both plus and minus strands in vitro. H4

deletion and site-specific alterations confirmed that H4 participates in accumulation of TCV, and demonstrated the importance of the terminal loop, internal asymmetric loop, and upper and lower stems in H4 function. The sequence that links H4 with H4a was also critical as demonstrated by elimination of detectable TCV accumulation when five consecutive adenylates were deleted. Since accumulation was partially restored when three adenylates were converted to uridyates, this suggests that the region may be important to spatially position H4 for correct function.

Insertion of H4 into a poorly replicating, artificial subviral RNA construct (CT) led to enhanced accumulation of subviral RNA monomers, suggesting that H4 functions during TCV replication, although a translational role cannot be ruled out. The inability of TT constructs to accumulate and weak enhancement of CT by H4 may reflect recently discovered complex requirements for subviral RNA accumulation, including a need for a conformational switch to apparently inactivate newly synthesized plus strands (Zhang et al., 2006, in press, submitted for publication). CT with wt or mutant H4 did not generate detectable levels of dimers (Fig. 4B), which is consistent with previous studies of the satC M1H enhancer, whose presence also correlated with a substantial decrease in the level of satC dimers (Nagy et al., 1999). The mechanism underlying the involvement of H4 and M1H in dimer accumulation remains unknown. Some deletions in the satC 5' region also greatly increased dimer levels while substantially reducing levels of monomers (Carpenter et al., 1991; Simon et al., 1988). This led to the suggestion that, once dimers are formed from reinitiation of synthesis by the RdRp before release of the newly synthesized strand, monomers and dimers accumulate independently of each other and may not share the same *cis*-requirements for replication. H4 (and M1H) inhibition of dimer accumulation could therefore reflect either a reduction in initial dimer formation or a suppression of dimer replication.

Previous studies indicated that TCV H4(-) is a recombination hotspot (in the absence of an adjacent hairpin) leading to the suggestion that H4 might serve as a *cis*-replication element primarily in its minus-sense orientation during plus-strand synthesis (Carpenter et al., 1995). Our current findings that H4(-) is bound by p88 in vitro and can function as an enhancer in vitro provides additional support for H4(-) contributing to TCV accumulation by helping to attract the RdRp to minus-strands. How a 5' proximal element (on minus-strands) might enhance transcription from the distal 3' end was recently elucidated for the minus-sense, dual hairpin enhancer/RdRp binding element [SL1-III(-) and SL2-III(-)] of viruses in the Tombusvirus genus (Panavas and Nagy, 2005). A sequence linking the two hairpins acts as a bridge to the 3' promoter by pairing with sequence near the 3' end. Several possible bridging sequences also exist between H4(-) and 3' terminal sequences, which are currently being investigated.

Based on strand-specific disruptions in Tombusviral RNAs assayed in vivo (Ray and White, 2003) and ability of only minus-sense SL1-III and SL2-III to enhance transcription by the RdRp from a minus-sense promoter in vitro (Panavas and Nagy,

2003; Panavas and Nagy, 2005), SL1-III and SL2-III were proposed to function in their minus-sense orientations. However, inverting the hairpins did not decrease accumulation of constructs *in vivo* compared with constructs containing the hairpins in their forward orientations (Ray and White, 2003) and both plus- and minus-sense stem-loops bound RdRp *in vitro*, although affinity was higher for the minus-sense enhancers (Panavas and Nagy, 2005). These results suggest that the Tombusvirus enhancers may also function in their plus-sense orientation. H4(+) is just upstream from four 3' terminal hairpins conserved in satC, TCV, CCFV, and the related carmovirus *Japanese iris necrosis virus*, which are important for initiation of satC minus-strand synthesis (Zhang et al., 2004, 2006) and which appear to play similar roles in TCV accumulation (J. McCormack and A. E. Simon, unpublished data). Our current results support an important role for H4(+) since maintaining the structure of H4(+) (construct M8) resulted in greater TCV accumulation than maintaining the H4(-) structure (construct M9). However, preserving H4(-) while disrupting H4(+) led to greater TCV accumulation when compared with simultaneous disruptions of both structures (constructs M5 and M6), suggesting that both H4(+) and H4(-) function in TCV genomic RNA replication.

Both H4 orientations had similar binding affinities for p88, which were substantially greater than the binding affinities of two TCV core promoters. This suggests that H4 may function in the initial binding of the RdRp to plus- and minus-strands during viral replication. Alternatively, it is possible that the weak interaction of the Pr (and CCS) with the RdRp reflects a requirement for additional upstream elements for efficient promoter function (Zhang et al., *in press*). Strong RdRp binding to H4(+) and H4(-) was reflected in enhanced p88 transcription of constructs containing core promoters and either H4(-) or H4(+) *in vitro*. Putative communication between H4 and other elements is suggested by the negative effect of mutations in the H4 terminal and internal loops on TCV accumulation that was not reflected in either enhancer activity or RdRp binding. The detrimental effects caused by disruption of the upper stem suggest that correct H4 folding is essential for enhancer function and the related ability to bind RdRp.

Interestingly, H4(+) was a much weaker enhancer of Pr activity compared with H4(-) transcriptional enhancement of the linear minus-sense CCS promoter. This may reflect that correct function of H4(+) in the genomic RNA requires the downstream H4a/H4b/H5 elements. The satC 3' region consisting of H4a/H4b/H5 and Pr was recently found to undergo a conformational switch from a pre-active structure that does not apparently contain these hairpins to an active structure where these hairpins are needed to direct minus-strand synthesis (Zhang et al., 2006, *submitted for publication*). Since TCV genomic RNA is translated, a similar conformational switch could convert a translation-active form of the template to one that is replication-active. The location of H4(+) proximal to the 3' hairpins leads to the following proposal for H4(+) function in minus-strand synthesis: an interaction between the H4(+) terminal loop and a downstream sequence helps to maintain the translation-active structure. RdRp binding to H4(+) disrupts

this interaction leading to a conformational switch to a replication-active form. The role of the RdRp in mediating such a switch may be similar to the binding of poliovirus-encoded 3CD to a cloverleaf structure near the 5' end of the poliovirus genome that causes translation to cease and replication to commence (Gamarnik and Andino, 1998). In *Alfalfa mosaic virus*, CP binding to 3' viral elements also causes a switch from the translation to the replication form of the RNA (Olsthoorn et al., 1999). The structural and functional similarity between TCV H4 and satC M1H suggests that M1H assumes the role of H4 in attracting the RdRp to plus- and minus-strand satellite templates and may also help mediate the plus-strand conformational switch.

Materials and methods

RNA solution structure probing

Plus-strand transcripts of TCV were synthesized using T7 RNA polymerase from *Sma*I-linearized pTCV66, which contains a T7 RNA polymerase promoter upstream of TCV full-length plus-strand sequence (Oh et al., 1995). Minus-strand transcripts were synthesized from *Xba*I-linearized pT7TCV(-) containing a T7 RNA polymerase promoter upstream of the TCV full-length minus-strand sequence (Carpenter et al., 1995). Solution structure probing was performed as previously described (Carpenter et al., 1995; Wang et al., 1999). Briefly, TCV plus- and minus-strand transcripts (11 µg) were mixed with 110 µg of yeast tRNA and 675 µl of modification buffer (70 mM HEPES, pH 7.5, 10 mM MgCl₂, 0.1 mM EDTA, 100 mM KCl). The mixture was heated to 90 °C, slowly cooled to 35 °C, and incubated at 25 °C for 20 min. Fifty-microliter samples of RNA were added to an equal volume of modification buffer containing either no additional reagents (control) or one of the following: 1% (v/v) dimethylsulfate (DMS; Sigma), 0.05 units of RNase T1 (Ambion), 0.03 units of RNase V1 (Ambion), or 0.04 units of RNase A (Ambion). After 10 and 20 min treatment with DMS, or 5 and 10 min treatments with enzymes, reactions were phenol extracted and ethanol precipitated followed by primer extension using 1 pmol of oligo13 (oligonucleotides used in this study are listed in Table 1) for plus-strand TCV or oligo3773(-) for minus-strand TCV, MMLV reverse transcriptase and [α -³⁵S]-radiolabeled dATP. Samples were subjected to electrophoresis on a 6% Long-Ranger sequencing gel (FMC BioProducts), followed by autoradiography.

Construction of TCV mutants

Construct M1 was generated by a three-step method. First, a 5' PCR fragment was obtained using primers Oligo3241F and OligoH4del with pTCV66 as template. Second, a 3' PCR fragment was obtained using primers Oligo3911(-) and Oligo4005R (Song and Simon, 1994) with pTCV66 as template. Third, both the 5' PCR fragment and the 3' PCR fragment were gel purified, ligated together using T4 DNA ligase, and used as template to amplify the ligation product by PCR using end primers Oligo3241F and Oligo4005R. The

resulting PCR products were digested with *MscI* and *SpeI*, gel purified and used to replace the *MscI*–*SpeI* segment of pTCV66. Other constructs (from M2 to M17) were generated as with M1, except that OligoH4del was replaced with primers OligoC3891G, OligoG3876C, OligoG3876C, Oligo3873, Oligo3873, Oligo3873, Oligo3873, OligoL2UUR, OligoPA5MUT, OligoRA5 mut, Oligo3892(+), OligoPA5MUT, Oligo3869, Oligo3869, Oligo3869, respectively, and Oligo3911 (–) was replaced with Oligo3892(–), Oligo3877(–), Oligo3877/3905, OligoTAat, OligoatTA, OligoTATA, OligoGtGt, OligoCaC, OligoL2UUF, Oligo3892(–), Oligo3911(–), Oligo3911 (–), OligoPRA5 mut, OligoCC, OligoGG, OligoGC, respectively. All clones were confirmed by sequencing.

Construct TT, TT-H4 and TT-H4_{M11} were obtained as follows. The 5' PCR fragments were generated using primers OligoT70001 and OligoTCV180R with pTCV66 as template. The 3' PCR fragment of TT was obtained using primers OligoCxdelH4 and Oligo8 with M1 as template. The 3' fragments of TT-H4 and TT-H4_{M11} were obtained using primers OligoCXgg and Oligo8, with pTCV66 and M11 as templates, respectively. Both the 5' and 3' fragments were treated with *Bam*HI, gel purified, ligated together, and cloned into *Sma*I-digested pUC19. Construct CT, CT-H4 and CT-H4_{M11} were generated as with TT and its derivatives except that the 5' PCR fragments were obtained using primers OligoT7C5 and OligosatC178R with pT7C(+) containing full-length satC cDNA as template (Song and Simon, 1994). All clones were confirmed by sequencing.

Pr-link1, Pr-link1-Rd1, Pr-link1-H4(+), Pr-link1-H4(+)_{M5}, Pr-link1-H4(+)_{M10}, and Pr-link1-H4(+)_{M11} were obtained by PCR using pTCV66 as template with 3' end primer Oligo8 and one of the following 5' primers: OligoT7ckF, OligoT7RdF, OligoT7H4F, OligoT7M5F, OligoT7M10F, and OligoT7L2 mF. CCS-link2, CCS-link2-Rd2, CCS-link2-H4(–), CCS-link2-H4(–)_{M5}, CCS-link2-H4(–)_{M10}, and CCS-link2-H4(–)_{M11} were obtained by PCR using pTCV66 as template with 3' end primer Oligo0001 and one of the following 5' primers: OligoT7ckR, OligoT7RdR, OligoT7H4R, OligoT7M5R, OligoT7M10R, and OligoT7L2 mR.

Protoplast inoculation

TCV RNAs were transcribed using T7 RNA polymerase from pTCV66 (Oh et al., 1995) and its derivatives. Protoplasts (5×10^6) prepared from callus cultures of *Arabidopsis thaliana* ecotype Col-0 were inoculated with 20 µg of plus-strand TCV transcripts with or without 2 µg of subviral RNA transcripts (TT, CT or their derivatives) as described previously (Kong et al., 1997). Total RNAs were extracted from protoplasts at 40 hpi as described (Wang and Simon, 1997).

Northern blot hybridization

Total RNAs were denatured with formamide and separated by non-denaturing agarose gel electrophoresis as previously described (Wang and Simon, 1997). Plus-strand RNAs were probed with [γ -³²P] ATP-labeled Oligo13 complementary to

positions 3950 to 3970 of TCV genomic RNA. Minus-strand RNAs were probed with [α -³²P] UTP-labeled oligonucleotide complementary to positions 3501 to 3664 of TCV minus-strands.

In vitro RNA transcription using purified recombinant TCV p88

PCR-amplified DNA were used as templates for transcription by T7 polymerase. After phenol/chloroform extraction, unincorporated nucleotides were removed by repeated ammonium acetate/isopropanol precipitation (Song and Simon, 1994; Nagy et al., 1997). The plasmid expressing TCV p88 was a generous gift of P. D. Nagy (U of Kentucky). Expression and purification of p88 from *E. coli* were carried out as previously described (Rajendran et al., 2002). *In vitro* RdRp assays were also performed as previously described (Nagy et al., 1999; 2001). Briefly, 3 µg of purified RNA template was added to a 25-µl reaction mixture containing 50 mM Tris–HCl (pH 8.2), 100 mM potassium glutamate, 10 mM MgCl₂, 10 mM dithiothreitol, 1 mM each of ATP, CTP, GTP, 0.01 mM UTP, 10 µCi [α -³²P] UTP (Amersham) and 2 µg of p88. The conditions for assays were modified to keep the molar ratios of RNA templates to p88 identical among all samples. After 90-min incubation at 20 °C, 1 µg of yeast tRNA was added and the mixture was subjected to phenol–chloroform extraction and ammonium acetate–isopropanol precipitation. For some of the reactions, half of the RdRp products were treated with S1 nuclease as described previously (Nagy et al., 1998). Products synthesized using CCS-link2-H4(–) were either treated with S1 nuclease or heated to 90 °C, slowly cooled to 25 °C, and then treated with S1. Radiolabeled products were analyzed by denaturing 8 M urea–5% polyacrylamide gel electrophoresis followed by autoradiography. Gels were stained with ethidium bromide, photographed, and dried, followed by analysis with a phosphorimager as described (Nagy et al., 1997). Data were normalized based on the number of template-directed radioactive UTP incorporated into the RdRp products and the molar amount of template RNA used in the RdRp reaction.

p88 binding assays

T7 RNA polymerase was used to transcribe *Sma*I-linearized pT7D(–), which contains a T7 RNA polymerase promoter upstream of satD full-length minus-strand sequence (Song and Simon, 1994), in the presence of 5 mM each of ATP, CTP, GTP, 0.05 mM UTP, and 10 µCi [α -³²P] UTP (Amersham). Approximately 10 ng of labeled RNAs, together with unlabeled competitor RNAs, were mixed with 1 µg of p88 in binding buffer (50 mM Tris–HCl [pH 8.2], 10 mM MgCl₂, 10 mM dithiothreitol, 10% glycerol, and 2 U of RNase inhibitor [Invitrogen]) (Rajendran et al., 2002). After incubating for 25 min at 25 °C, the samples were analyzed by electrophoresis on native 1% agarose gels. Electrophoresis conditions were 100 V for 2 h at 4 °C in 0.5× TBE buffer. The gels were dried and followed by autoradiography.

Acknowledgments

Funding was provided by grants from the U.S. Public Health Service (GM61515-01) and the National Science Foundation (MCB-0086952) to AES.

References

- Buck, K.W., 1996. Comparison of the replication of positive-stranded RNA viruses of plants and animals. *Adv. Virus Res.* 47, 159–251.
- Carpenter, C.D., Simon, A.E., 1998. Analysis of sequences and putative structures required for viral satellite RNA accumulation by in vivo genetic selection. *Nucleic Acids Res.* 26, 2426–2432.
- Carpenter, C.D., Cascone, P.J., Simon, A.E., 1991. Formation of multimers of linear satellite RNAs. *Virology* 183, 586–594.
- Carpenter, C.D., Oh, J.-W., Zhang, C., Simon, A.E., 1995. Involvement of a stem-loop structure in the location of junction sites in viral RNA recombination. *J. Mol. Biol.* 245, 608–622.
- Cascone, P.J., Haydar, T., Simon, A.E., 1993. Sequences and structures required for RNA recombination between virus-associated RNAs. *Science* 260, 801–805.
- Cheng, C.P., Panavas, T., Luo, G., Nagy, P.D., 2005. Heterologous RNA replication enhancer stimulates in vitro RNA synthesis and template-switching by the carmovirus, but not by the tombusvirus, RNA-dependent RNA polymerase: implication for modular evolution of RNA viruses. *Virology* 341, 107–121.
- Chapman, R.M., Kao, C.C., 1999. A minimal RNA promoter for minus-strand RNA synthesis by the brome mosaic virus polymerase complex. *J. Mol. Biol.* 286, 709–720.
- Dreher, T.W., 1999. Functions of the 3'-untranslated regions of positive strand RNA viral genomes. *Annu. Rev. Phytopathol.* 37, 151–174.
- Duggal, R., Lahser, F.C., Hall, T.C., 1994. Cis-Acting sequences in the replication of plant viruses with plus-sense RNA genomes. *Annu. Rev. Phytopathol.* 32, 287–309.
- Fabian, M.R., Na, H., Ray, D., White, K.A., 2003. 3'-Terminal RNA secondary structures are important for accumulation of Tomato bushy virus DI RNAs. *Virology* 313, 567–580.
- Gamarnik, A.V., Andino, R., 1998. Switch from translation to RNA replication in a positive-stranded RNA virus. *Genes Dev.* 12, 2293–2304.
- Goebel, S.J., Hsue, B., Dombrowski, T.F., Masters, P.S., 2004. Characterization of the RNA components of a putative molecular switch in the 3' untranslated region of the murine coronavirus genome. *J. Virol.* 78, 669–682.
- Guan, H., Carpenter, C.D., Simon, A.E., 2000. Analysis of cis-acting sequences involved in plus-strand synthesis of a TCV-associated satellite RNA identifies a new carmovirus replication element. *Virology* 268, 345–354.
- Hacker, D.L., Petty, I.T.D., Wei, N., Morris, T.J., 1992. Turnip crinkle virus genes required for RNA replication and virus movement. *Virology* 186, 1–8.
- Kim, Y.N., Makino, S., 1995. Characterization of a murine coronavirus defective interfering RNA internal cis-acting replication signal. *J. Virol.* 69, 4963–4971.
- Kong, Q., Oh, J.-W., Simon, A.E., 1995. Symptom attenuation by a normally virulent satellite RNA of Turnip crinkle virus is associated with the coat protein open reading frame. *Plant Cell* 7, 1625–1634.
- Kong, Q., Oh, J.-W., Carpenter, C.D., Simon, A.E., 1997. The coat protein of Turnip crinkle virus is involved in subviral RNA-mediated symptom modulation and accumulation. *Virology* 238, 478–485.
- Lai, M.M.C., 1998. Cellular factors in the transcription and replication of viral RNA genomes: a parallel to DNA-dependent RNA transcription. *Virology* 244, 1–12.
- Li, W.-Z., Qu, F., Morris, T.J., 1998. Cell-to-cell movement of turnip crinkle virus is controlled by two small open reading frames that function in trans. *Virology* 244, 405–416.
- McCormack, J., Simon, A.E., 2004. Biased hypermutagenesis of an RNA virus associated with mutations in an untranslated hairpin. *J. Virol.* 78, 7813–7817.
- Nagy, P.D., Carpenter, C.D., Simon, A.E., 1997. A novel 3'-end repair mechanism in an RNA virus. *Proc. Natl. Acad. Sci. U.S.A.* 94, 1113–1118.
- Nagy, P.D., Zhang, C., Simon, A.E., 1998. Dissecting RNA recombination in vitro: role of RNA sequences and the viral replicase. *EMBO J.* 17, 2392–2403.
- Nagy, P.D., Pogany, J., Simon, A.E., 1999. RNA elements required for RNA recombination function as replication enhancers in vitro and in vivo in a plus-strand RNA virus. *EMBO J.* 18, 5653–5665.
- Nagy, P.D., Pogany, J., Simon, A.E., 2001. In vivo and in vitro characterization of an RNA replication enhancer in a satellite RNA associated with turnip crinkle virus. *Virology* 288, 315–324.
- Oh, J.-W., Kong, Q., Song, C., Carpenter, C.D., Simon, A.E., 1995. Open reading frames of turnip crinkle virus involved in satellite symptom expression and incompatibility with Arabidopsis ecotype Dijon. *Mol. Plant-Microb. Interact.* 8, 979–987.
- Olsthoorn, R.C., Mertens, S., Brederode, F.T., Bol, J.F., 1999. A conformational switch at the 3' end of a plant virus RNA regulates viral replication. *EMBO J.* 18, 4856–4864.
- Panavas, T., Nagy, P.D., 2003. The RNA replication enhancer element of tombusvirus contains two interchangeable hairpins that are functional during plus-strand synthesis. *J. Virol.* 77, 258–269.
- Panavas, T., Nagy, P.D., 2005. Mechanism of stimulation of plus-strand synthesis by an RNA replication enhancer in a tombusvirus. *J. Virol.* 79, 9777–9785.
- Panaviene, Z., Panavas, T., Serva, S., Nagy, P.D., 2004. Purification of the Cucumber necrosis virus replicase from yeast cells: role of coexpressed viral RNA in stimulation of replicase activity. *J. Virol.* 78, 8254–8263.
- Panaviene, Z., Panavas, T., Nagy, P.D., 2005. Role of an internal and two 3-terminal RNA elements in assembly of tombusvirus replicase. *J. Virol.* 79, 10608–10618.
- Pogany, J., Fabian, M.R., White, K.A., Nagy, P.D., 2003. A replication silencer element in a plus-strand RNA virus. *EMBO J.* 22, 5602–5611.
- Rajendran, K.S., Pogany, J., Nagy, P.D., 2002. Comparison of Turnip crinkle virus RNA-dependent polymerase preparations expressed in *Escherichia coli* or derived from infected plants. *J. Virol.* 76, 1707–1717.
- Ray, D., White, K.A., 1999. Enhancer-like properties of an RNA element that modulates Tombusvirus RNA accumulation. *Virology* 256, 162–171.
- Ray, D., White, K.A., 2003. An internally located RNA hairpin enhances replication of Tomato bushy stunt virus RNAs. *J. Virol.* 77, 245–257.
- Simon, A.E., Howell, S.H., 1986. The virulent satellite RNA of Turnip crinkle virus has a major domain homologous to the 3' end of the helper virus genome. *EMBO J.* 5, 3423–3428.
- Simon, A.E., Engel, H., Johnson, R.P., Howell, S.H., 1988. Identification of regions affecting virulence, RNA processing and infectivity in the virulent satellite of Turnip crinkle virus. *EMBO J.* 7, 2645–2651.
- Song, C., Simon, A.E., 1994. RNA-dependent RNA polymerase from plants infected with turnip crinkle virus can transcribe (+)- and (–)-strands of virus-associated RNAs. *Proc. Natl. Acad. Sci. U.S.A.* 91, 8792–8796.
- Song, C., Simon, A.E., 1995. Requirement of a 3'-terminal stem-loop in in vitro transcription by an RNA dependent RNA polymerase. *J. Mol. Biol.* 254, 6–14.
- Stupina, V., Simon, A.E., 1997. Analysis in vivo of turnip crinkle virus satellite RNA C variants with mutations in the 3'-terminal minus-strand promoter. *Virology* 238, 470–477.
- Turner, R.L., Buck, K.W., 1999. Mutational analysis of cis-acting sequences in the 3'- and 5'-untranslated regions of RNA2 of red clover necrotic mosaic virus. *Virology* 253, 115–124.
- Wang, J., Simon, A.E., 1997. Analysis of the two subgenomic RNA promoters for turnip crinkle virus in vivo and in vitro. *Virology* 232, 174–186.
- Wang, J., Simon, A.E., 1999. Symptom attenuation by a satellite RNA in vivo is dependent on reduced levels of virus coat protein. *Virology* 259, 234–245.
- Wang, J., Carpenter, C.D., Simon, A.E., 1999. Minimal sequence and structural requirements for a subgenomic RNA promoter for turnip crinkle virus. *Virology* 253, 327–336.
- Zhang, J., Simon, A.E., 2005. Importance of sequence and structural elements within a viral replication repressor. *Virology* 333, 301–315.
- Zhang, G., Zhang, J., Simon, A.E., 2004. Repression and derepression of minus-strand synthesis in a plus-strand RNA virus replicon. *J. Virol.* 78, 7619–7633.
- Zhang, G., Zhang, J., George, A.T., Baumstark, T., Simon, A.E., 2006.

- Conformational changes involved in initiation of minus-strand synthesis of a virus-associated RNA. *RNA* 12, 147–162.
- Zhang, J., Zhang, G., McCormack, J.C., Simon, A.E., in press. Evolution of Virus-Derived Sequences for High Level Replication of a subviral RNA. *Virology*.
- Zhang, J., Zhang, G., Guo, R., Shapiro, B.A., Simon, A.E., submitted for publication. A pseudoknot in a pre-active form of a viral RNA is part of a structural switch activating minus-strand synthesis. *J. Virol.*
- Zuker, M., 2003. Mfold web server for nucleic acid folding and hybridization prediction. *Nucleic Acids Res.* 31, 3406–3415.